

# Revisiting the crystal electric field of P2- $\text{Na}_x\text{CoO}_2$ for the intermediate spin state of $\text{Co}^{3+}$

G. J. Shu<sup>1</sup> and F. C. Chou<sup>1,2\*</sup>

<sup>1</sup>Center for Condensed Matter Sciences, National Taiwan University, Taipei 10617, Taiwan and

<sup>2</sup>National Synchrotron Radiation Research Center, Hsinchu 30076, Taiwan

(Dated: November 25, 2016)

The magnetic moment per  $\text{Co}^{4+}$  of P2( $\gamma$ )-type  $\text{Na}_x\text{CoO}_2$  in Curie-Weiss metal regime is revisited and examined under a newly proposed modification of the octahedral crystal electric field (CEF). The proposed model explains the origin of the existence of the intermediate state  $S=1$  for  $\text{Co}^{3+}$  through an exciton-like elementary excitation of the narrow gap between the split  $e_g$  and  $t_{2g}$  groups. The  $\text{CoO}_2$  layer is proposed to be constructed from the tilted edge-sharing square-planar  $\text{CoO}_2$  chains with inter-chain coupling. The square-planar CEF of  $\text{CoO}_2$  requires covalent bond formation between Co and the four in-plane neighboring oxygens, while the oxygens sitting in the neighboring chains can be viewed as apical oxygens of low effective charge for a  $\text{CoO}_6$  pseudo-octahedron. The reason why angle-resolved photoemission spectroscopy (ARPES) failed to observe the local-density approximation (LDA) predicted  $e'_g$  hole pockets at  $k_z=0$  and the reversed order of the  $t_{2g}$  splittings between LDA and CEF calculations can also be resolved using the proposed model.

PACS numbers: 71.70.Ch; 71.70.Ej; 75.30.Cr; 71.28.+d

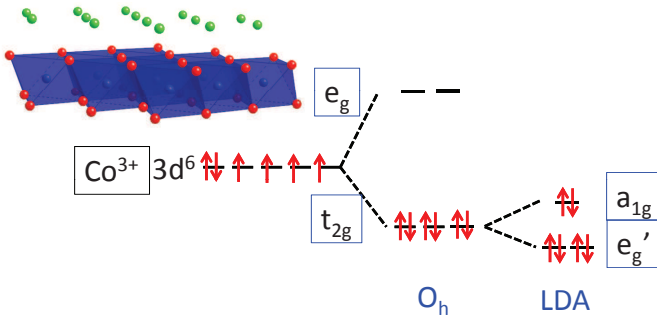


FIG. 1. (color online) The crystal structure of  $\text{Na}_x\text{CoO}_2$  is presented with the  $\text{CoO}_2$  and Na layers in the space group  $P6_3/mmc$ . The conventional electronic configuration of  $\text{Co}^{3+}$  ( $3d^6$ ) in an octahedral crystal field splits into  $e_g - t_{2g}$  groups, and the additional splitting of  $t_{2g}$  ( $e'_g - a_{1g}$ ) is due to trigonal distortion. In contrary to the spectrum of lower  $a_{1g}$  predicted from the CEF calculation, the  $a_{1g}$  is higher based on LDA calculations.<sup>1,2</sup>

Layered P2-type (or  $\gamma$ -type)  $\text{Na}_x\text{CoO}_2$  is an important class of material for both fundamental and applied aspects, e.g., it is a good candidate thermoelectric material with a high thermoelectric figure-of-merit (ZT) at high temperature;<sup>3</sup> has a great similarity to the important battery cathode electrode material  $\text{Li}_x\text{CoO}_2$ ;<sup>4</sup> has superconductivity, as observed in  $\text{Na}_{1/3}\text{CoO}_2$  after hydration;<sup>5</sup> and has an intriguing Curie-Weiss metal behavior as a strongly correlated electron material.<sup>6</sup> The crystal structure of  $\text{Na}_x\text{CoO}_2$  can be viewed as a Na layer sandwiched between  $\text{CoO}_2$  triangular lattice layers as illustrated in Fig. 1. A 2D triangular lattice of  $\text{CoO}_2$  formed by the closely packed  $\text{CoO}_6$  octahedra is commonly observed in many cobalt oxide compounds in contrast to the high  $T_c$  cuprate materials, which contain a 2D square lattice of  $\text{CuO}_2$ . The  $\text{CoO}_2$  layer has been the basic building block of many layered cobalt oxide compounds, including  $\text{Na}_x\text{CoO}_2$ ,  $\text{Pb}_2\text{Sr}_2\text{Co}_2\text{O}_y$ , and  $\text{Co}_3\text{Co}_4\text{O}_9$ , of various

types of staging and the unavoidable incommensurability is due to layer mismatch.<sup>7</sup> The physical properties of materials with a hole-doped  $\text{CoO}_2$  layer have often been interpreted from the mixed valence of  $\text{Co}^{3+}$  and  $\text{Co}^{4+}$ . However, the early d-orbital energy levels for Co under the octahedral crystal field assumption (see Fig. 1) cannot be used to reasonably interpret the Curie-Weiss metal behavior, especially concerning the puzzling questions of why the theoretically predicted  $e'_g$  hole pockets have not been observed experimentally, and why the  $t_{2g}$  splitting ( $a_{1g} - e'_g$ ) is reversed between predictions from LDA and CEF calculations.<sup>2,8</sup>

The existence of an intermediate spin ( $S=1$ ) for  $\text{Co}^{3+}$  has been proposed from the ellipsometry experimental results for  $\text{Na}_{0.82}\text{CoO}_2$ .<sup>9</sup> Daghofer *et al.* proposed that Hund's rule coupling across a narrow gap between the split  $e_g$  and  $t_{2g}$  groups could permit the existence of  $S=1$  within the proposed spin-orbit-polaron model, i.e., the intermediate spin (IS) state of  $S=1$  for  $\text{Co}^{3+}$  may exist in addition to the original low spin (LS) state of  $S=0$ .<sup>10</sup> However, in view of the large gap in  $\Delta$  of  $\sim 1$  eV between  $e_g - t_{2g}$ ,<sup>11</sup> it is difficult to construct one octahedral CEF that has an actual severe distortion. That is, the oxygens must be removed from the original apical positions, which is structurally or chemically nearly impossible due to the  $\text{CoO}_2$  layer formed by the closely packed edge-sharing octahedra. In addition, the energy levels of  $t_{2g}$  splitting predicted from the *ab initio* calculations are strangely reversed relative to the CEF prediction.<sup>2</sup> Landron *et al.* have carefully examined this issue but failed to uncover connections with the metal-ligand hybridization, the long-range crystalline field, the screening effects, and the orbital relaxation; the tentative conclusion still vaguely points to the mixing of  $e_g$  and  $t_{2g}$ .<sup>2</sup>

We have revisited this issue experimentally through the analysis of the effective magnetic moment for a series of  $\text{Na}_x\text{CoO}_2$  samples in the Curie-Weiss metal regime.

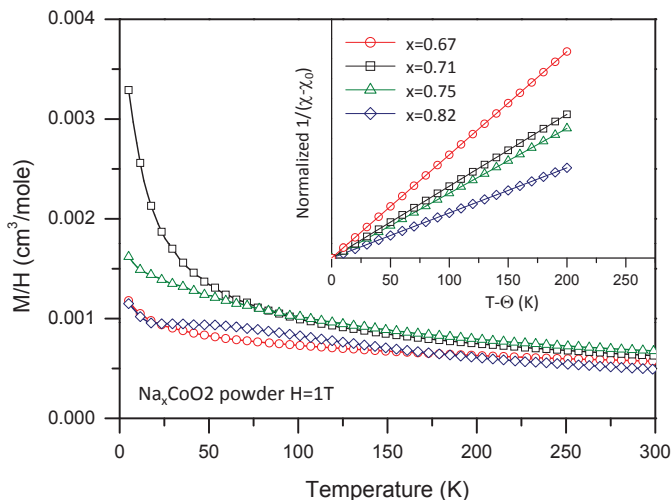


FIG. 2. (color online) Average spin susceptibilities of  $\text{Na}_x\text{CoO}_2$  ( $x=0.67-0.82$ ) in a 1 Tesla applied field. The inset shows normalized  $1/(\chi-\chi_0)$  vs.  $(T-\Theta)$  to illustrate the  $x$ -dependence of the Curie constant by the different slopes corresponding to  $1/C$ .

TABLE I. Curie-Weiss law,  $\chi(T) = \chi_0 + C/(T - \Theta)$ , fitting for polycrystalline samples of  $\text{Na}_x\text{CoO}_2$  in an applied field  $H=1$  Tesla.

$x$	0.67	0.71	0.75	0.82
fitting range	60-300K	65-300K	60-300K	125-300K
$\chi_0$ ( $\text{cm}^3/\text{mole}$ )	0.0004(5)	0.0003(7)	0.0003(6)	0.0001(5)
$C$ ( $\text{cm}^3\text{-K}/\text{mole}$ )	0.0675(5)	0.1082(1)	0.1311(3)	0.1423(2)
$\Theta$ (K)	-103.5(7)	-70.2(5)	-106.1(7)	-102.5(3)
$\mu_{eff}$ ( $\mu_B$ per Co)	0.7350	0.9305	1.0243	1.0671
$\mu_{eff}$ ( $\mu_B$ per $\text{Co}^{4+}$ )	1.279	1.728	2.049	2.515
$\alpha$	-0.084*	0.00068	0.049	0.091

\*This value is unphysical, which implies that the itinerant contribution is no longer negligible.

Single crystal samples of  $\text{Na}_x\text{CoO}_2$  of  $x\sim 0.8$  were grown using the optical floating-zone method in an oxygen atmosphere. The Na contents of the single crystal samples were fine-tuned to  $x=0.67, 0.71, 0.75,$  and  $0.82$  using an electrochemical intercalation technique and verified with electron microprobe analysis (EPMA), within an error of  $\pm 0.01$ , as described previously.<sup>12</sup> Average spin susceptibility ( $\chi(T)=M/H$ ) data were acquired from a pulverized powder sample under an applied magnetic field of 1 Tesla in the temperature range of 5-300K, as shown in Fig. 2. The spin susceptibilities can be fitted satisfactorily with the Curie-Weiss law,  $\chi(T) = \chi_0 + C/(T - \Theta)$ , in the paramagnetic regime and are summarized in Table I. Assuming the amount of  $\text{Co}^{4+}$  ( $(t_{2g})^5$ ) with  $S=1/2$  can be determined directly from the Na content  $x$  without oxygen vacancies, it is expected that the  $\mu_{eff}$  values per  $\text{Co}^{4+}$  should be  $1.732 \mu_B$  with  $g=2$ . However, it is clear that except for the sample of  $x=0.71$ , the  $\mu_{eff}$  per  $\text{Co}^{4+}$  values are progressively and significantly higher than  $1.732 \mu_B$  for  $x > 0.71$ , as indicated in Table I. Similar results have also been reported consistently in all early published

works,<sup>6,13-15</sup> including for  $\text{Li}_x\text{CoO}_2$ , which has a similar  $\text{CoO}_2$  2D triangular lattice.<sup>4</sup> While a Na content higher than  $\sim 0.71$  is expected to contain a lower level of  $\text{Co}^{4+}$  and less doped itinerant holes, the increasing Curie constant remains unclear.

While the  $\text{CoO}_2$  layer of  $\text{Na}_x\text{CoO}_2$  has been viewed as closely packed edge-sharing octahedra that forms a 2D triangular lattice, the distortion from the flattened  $\text{CoO}_2$  layer along the rhombohedral (111) axis requires the distortion of octahedral CEF, whereupon the  $t_{2g}$  degeneracy is lifted. The octahedral distortion has been reflected on the subtle difference of Co-O bond lengths and O-Co-O bond angles in  $\text{CoO}_6$  through synchrotron X-ray structure refinement before.<sup>16</sup> In the crystal field theory for elongated octahedral CEF, as illustrated in Fig. 3,  $e_g$  splits into  $b_{1g}-a_{1g}$  and  $t_{2g}$  splits into  $b_{2g}-e'_g$ , where “a/b”, “e”, and “t” denote single, double, and triple degeneracy in the convention of group theory, respectively.<sup>17</sup> The two groups of the  $e_g$  doublet and  $t_{2g}$  triplet have a large gap of a  $\Delta_{oct}$  of  $\sim 1$  eV, and the elongation of the apical Co-O distance lifts the degeneracy of both  $e_g$  and  $t_{2g}$  by lowering the z-related levels within each group. The extreme case of such a distortion can be observed in the square-planar CEF that is derived by removing apical oxygens to infinity, which lowers the z-related levels significantly, as demonstrated in Fig. 3(d). However, since the first published LDA band calculation for  $\text{Na}_x\text{CoO}_2$ , the  $t_{2g}$  splitting has been commonly mislabeled as  $a_{1g}-e'_g$  in the physics community (see Fig. 1),<sup>1</sup> and  $a_{1g} = (d_{xy} + d_{yz} + d_{zx})/\sqrt{3}$  and  $e'_g = [(d_{zx} - d_{yz})/\sqrt{2}, (2d_{xy} - d_{yz} - d_{zx})/\sqrt{6}]$  after an axis transformation of the principal z-axis from the apical oxygen direction to the (111) direction in rhombohedral symmetry.<sup>2,8</sup> Note that the relative positions of the ligand does not change after axis transformation, and an identical  $t_{2g}$  splitting, as a result of octahedral CEF distortion, can be described for any selection of an axes system. The most common distortion in the rhombohedral symmetry description is the thickness change of the  $\text{CoO}_2$  layer, which can be roughly represented by a small elongation from the original perfect  $\text{CoO}_6$  octahedron.

If the  $\text{CoO}_2$  layer is viewed as closely packed edge-sharing octahedra, it is impossible to create one distorted octahedral CEF by adjusting the apical Co-O bond lengths alone, i.e., to create a distortion severe enough for both the  $e_g$  and  $t_{2g}$  groups to split wide and leave one small gap between them. Instead of assuming that the  $\text{CoO}_2$  layer which is composed of edge-sharing octahedra, we propose an alternative view; the  $\text{CoO}_2$  layer could be composed of edge-sharing square-planar  $\text{CoO}_2$  chains with nontrivial inter-chain coupling, as illustrated in Fig. 4. There are two main reasons to make such an assumption; the first is because the earlier view of octahedral CEF with trigonal distortion failed to provide a reasonable argument to allow the formation of a narrow gap between the  $e_g$  and  $t_{2g}$  groups, and the second is that each oxygen with two electrons missing from its  $2p$ -orbital can form, at most, two covalent bonds with

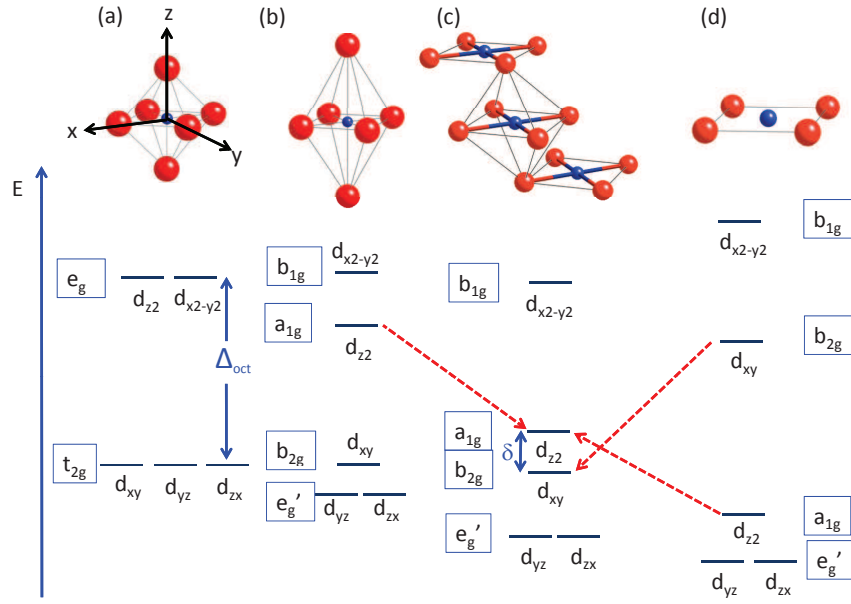


FIG. 3. (color online) The d-orbital energy splittings of a transition metal surrounded by oxygen ligands in (a) regular octahedral CEF in  $O_h$  symmetry, (b) octahedral CEF with principal z-axis elongation in  $D_{4h}$  symmetry, (c) the proposed CEF with weak effective charge at the apical ligand positions, and (d) the square-planar CEF in  $C_{4v}$  symmetry.<sup>17</sup>

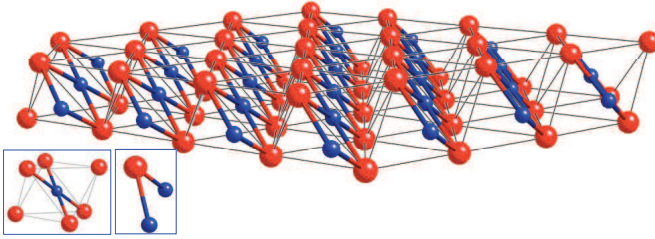


FIG. 4. (color online) The  $\text{CoO}_2$  plane can also be viewed as edge-sharing square-planar chains with inter-chain coupling instead of edge-sharing octahedra. The pseudo-octahedron of  $\text{CoO}_6$  and  $\text{Co-O-Co}$  at  $90^\circ$  are shown in the insets.

the neighboring Co atoms in a  $90^\circ$  coordination, as illustrated in the inset of Fig. 4. Chemically, it is impossible for oxygen to form three covalent bonds with the neighboring three Co atoms, as implied in the earlier octahedral picture.

The modified view of CEF is effectively in between an elongated octahedral CEF and a square-planar CEF. It is possible that the Co-O only has four covalent  $\sigma$ -bonds within each square-planar  $\text{CoO}_2$  unit, and the apical oxygens should not be viewed as individual ligands but as weak effective charges dressed by the neighboring edge-sharing chains, as illustrated in Fig. 4. The  $\text{CoO}_2$  plane originally assumed to be in edge-sharing octahedra is now viewed as edge-sharing square-planar chains with inter-chain coupling, i.e., all of the oxygens in each square-planar edge-sharing chain also serve as the effective apical oxygen for the neighboring square-planar  $\text{CoO}_2$  unit to form a pseudo-octahedron. The actual crystal field can now be understood as a unique octahedral CEF with apical oxygens of a much less effective charge. In fact

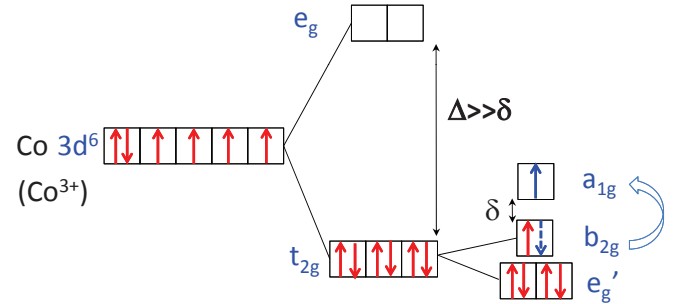


FIG. 5. (color online) The low spin (LS) state and intermediate spin (IS) state for  $\text{Co}^{3+}$  ( $3d^6$ ) derived from the proposed CEF. Thermal or strain energy at ambient temperature would allow activation between  $a_{1g}$ - $b_{2g}$  of the narrow gap  $\delta$  on the order of  $\sim 10$  meV.

similar energy splitting can also be generated through the additional magnetic couplings of  $J_{diag}$  and  $J'$  per polaron unit defined in the calculations by Daghofer *et al.*<sup>10</sup> Starting from the square-planar CEF, the effective charge of a distorted octahedral CEF may be formed when the  $a_{1g}$  ( $d_{z^2}$ ) level is raised slightly above the  $b_{2g}$  ( $d_{xy}$ ) level. A clear level inversion between  $a_{1g}$  and  $b_{2g}$  between the square-planar and elongated octahedral CEF occurs once the effective charge of the apical oxygen is properly tuned through the inter-chain coupling .

Following our proposed model, which leads to the possible existence of a narrow gap between the  $e_g$  and  $t_{2g}$  groups, i.e., the small gap ( $\delta$ ) between  $a_{1g}$ - $b_{2g}$  shown in Fig. 3(c), we may re-examine the spins of the 3d electrons in the Co ions. It is commonly accepted that the LS states of  $\text{Co}^{3+}$  ( $3d^6$ ) and  $\text{Co}^{4+}$  ( $3d^5$ ) are  $S=0$  and  $S=1/2$ , respectively. In the newly constructed CEF with

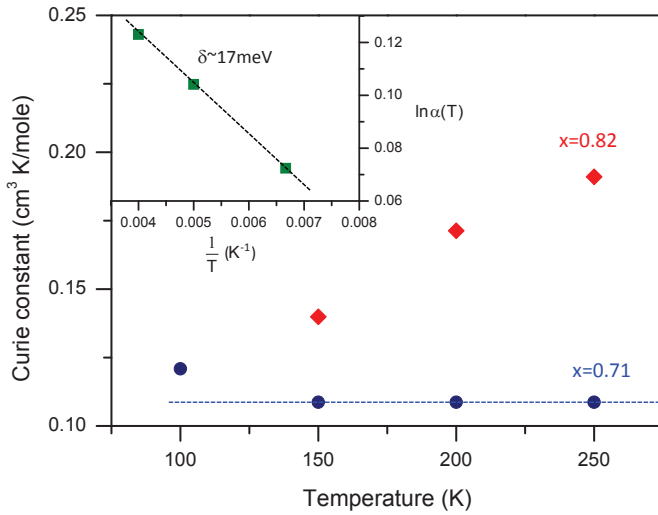


FIG. 6. (color online) Temperature dependence of Curie constants for  $x=0.82$  and  $0.71$ , where Curie-Weiss law fittings were performed using the selected temperature sections of  $\pm 50\text{K}$  centered between  $100\text{-}250\text{K}$ . The inset shows Arrhenius plot for the number of activated  $S=1$  state of  $\text{Co}^{3+}$  ( $\alpha(T)$ ) with activation energy ( $\delta$ ) between  $a_{1g} - b_{2g}$  fitted to be  $\sim 17$  meV.

a narrow gap between  $a_{1g}-b_{2g}$  of  $\sim 10$  meV,<sup>8</sup> the thermal or stain energy at ambient temperature would be sufficient to activate electrons from the filled  $b_{2g}$  to the empty  $a_{1g}$ , as illustrated in Fig. 5. In fact, Hund's rule coupling is an alternative description for the existence of IS state when the pairing energy is able to overcome the small CEF gap.<sup>10</sup> For the IS state ( $S=1$ ) of  $\text{Co}^{3+}$  generated through the activation process, the quantity and positions of  $S=1$  must fluctuate in a Boltzmann distribution of population and at random positions. It is reasonable to assume that the Curie constant should change as a function of temperature, i.e., increased  $S=1$  should be observed at higher temperatures because of increased  $S=1$  activation across the narrow  $a_{1g} - b_{2g}$  gap for  $\text{Co}^{3+}$ .

The Curie-Weiss law for the localized spins is an approximation of Brillouin function under the condition of  $\mu H/k_B T \ll 1$ , i.e., the Curie constant should be temperature independent at low field and high temperature regime. As a double check to the validity of the applied Curie-Weiss law fitting, the fitted Curie constant for  $x=0.71$  does show a temperature independent value at high temperature above  $\sim 150\text{K}$  (see Fig. 6), and only deviates at low temperature when the  $\mu H/k_B T \ll 1$  condition is violated. On the other hand, we find that the Curie constant has a subtle temperature dependence when the Curie-Weiss law is fitted using different temperature sections, especially for  $x=0.82$  as shown in Fig. 6. The temperature dependence of  $C(T)$  ( $C=N\mu_{eff}^2/3k_B$ ) could be coming from the  $N(T)$  through added number of localized spins, or from the  $\mu_{eff}(T)$  through added couplings that enhance the size of the magnetic moment of the localized spins effectively. T. Moriya has shown that the spin fluctuation of FM coupled itinerant electrons

in the strongly correlated system can also be described with a Curie's law defined in parallel to that of the localized spins.<sup>19</sup> While we cannot rule out that the observed Curie constant has contribution from the correlated itinerant electrons completely, especially from the RKKY type coupling of itinerant electrons to the localized spins of  $S=1/2$  for  $\text{Co}^{4+}$ ,<sup>20</sup> the impact of these couplings should be diminishing at higher temperature. However, the increasing  $C(T)$  as a function of temperature for  $x=0.82$  (see Fig. 6) does not support, or at least implies that the scenario of coupling enhanced effective moment cannot be the dominant factor. Quite the contrary, the increasing  $C(T)$  suggests that more localized spins are added to the system at higher temperature, which agrees with a picture that more spins of  $S=1$  are generated from the thermally activated IS state of  $\text{Co}^{3+}$ .

The confusing excess magnetic moment per  $\text{Co}^{4+}$  beyond  $S=1/2$  presented in Table I can now be analyzed quantitatively using the proposed model. Using  $\text{Na}_{0.82}\text{CoO}_2$  as an example, the Curie constant ( $C=N\mu_{eff}^2/3k_B$ ) has three possible contributions from the LS state of  $\text{Co}^{4+}$  with  $S=1/2$  ( $\mu_{\text{Co}^{4+}}^{LS}=1.732\mu_B$ ), the LS state of  $\text{Co}^{3+}$  with  $S=0$  ( $\mu_{\text{Co}^{3+}}^{LS}=0$ ), and the IS state of  $\text{Co}^{3+}$  with  $S=1$  ( $\mu_{\text{Co}^{3+}}^{IS}=2.828\mu_B$ ). Under the constraint of total  $N=N_{\text{Co}^{4+}}^{LS}+N_{\text{Co}^{3+}}^{LS}+N_{\text{Co}^{3+}}^{IS}$ , the  $\mu_{eff}$  per Co ion can be analyzed with a modified Curie-Weiss law ( $\chi = \chi_0 + \frac{C}{T-\Theta}$ ) of

$$C = \frac{N_{\text{Co}^{4+}}^{LS}(\mu_{\text{Co}^{4+}}^{LS})^2 + N_{\text{Co}^{3+}}^{LS}(\mu_{\text{Co}^{3+}}^{LS})^2 + N_{\text{Co}^{3+}}^{IS}(\mu_{\text{Co}^{3+}}^{IS})^2}{3k_B}$$

We may estimate the fraction ( $\alpha$ ) of  $\text{Co}^{3+}$  at the activated IS state ( $S=1$ ) at any instance from

$$\mu_{eff}^2 = (1 - 0.82) \times 1.732^2 + 0.82[(1 - \alpha) \times 0^2 + \alpha \times 2.828^2].$$

The fractions of  $\text{Co}^{3+}$  at  $S=1$ ,  $\alpha$ , is estimated to be nearly 9% under 1 Tesla in the temperature range of  $125\text{-}300\text{K}$  (see Table I), which quantitatively agrees with a description that at most one  $\text{Co}^{3+}$  in a Na di-vacancy formed  $\sqrt{13}a$  superlattice ( $1-\frac{11}{13}\sim 9\%$ ) is activated, i.e., for each di-vacancy formed supercell with 2  $\text{Co}^{4+}$  at the corners and 11  $\text{Co}^{3+}$  in the middle, only one of the  $\text{Co}^{3+}$  (random in time and position) is activated from  $S=0$  to  $S=1$ . In the meantime, there is almost no IS state activation for  $x=0.71$ , as indicated by the  $\alpha\approx 0$  value observed in Table I, which is reasonable because  $x=0.71$  has a smaller  $\sqrt{12}a$  superlattice size formed by mixed Na tri- and quadri-vacancies of larger  $\text{Co}^{4+}$  clusters.<sup>6,21</sup> We must note that the regular magnetic field strength does not provide enough Zeeman energy to keep the electron stabilized at the IS state of  $S=1$ ; however, the narrow gap activation process would keep a fixed amount of  $\text{Co}^{3+}$  ions at the IS state at random positions. In fact, such a narrow gap activation process is equivalent to an elementary excitation, similar to that of the quasiparticle excitation used as a method of energy transport in condensed matter without actual net charge transport.



The temperature dependence of Curie constant  $C(T)$  for  $x=0.82$  (Fig. 6) implies that the number of localized spins is raised at higher temperature, which is in accord with the proposed model of thermally activated IS state ( $S=1$ ) for  $\text{Co}^{3+}$ . Following the same quantitative analysis that extracts the fraction of  $\text{Co}^{3+}$  at  $S=1$ ,  $\alpha$ , the  $a_{1g} - b_{2g}$  gap (i.e.,  $\delta$  defined in Fig. 5) can be estimated from the fitting of activation energy of  $\alpha(T) \sim e^{(-\delta/k_B T)}$  in Arrhenius law, as shown in the inset of Fig. 6 with log scale. The activation energy for  $\text{Co}^{3+}$  activated from the ground state of  $S=0$  to the excited state of  $S=1$  between the narrow gap of  $a_{1g} - b_{2g}$  is fitted to be  $\delta \sim 17$  meV, which provides a reasonable order experimentally and is in agreement with that estimated from the crystal field calculation.<sup>8,10</sup>

The current model can also resolve the puzzling contradiction concerning why LDA calculations predicted  $e'_g$  hole pockets along  $\Gamma - K$  at  $k_z=0$  have never been observed in ARPES experiments.<sup>1,22</sup> A strong electronic correlation has been proposed to be responsible for the missing  $e'_g$  hole pockets, i.e., the  $e'_g$  band could be pushed below the Fermi level.<sup>8</sup> Based on our proposed CEF model, the absence of  $e'_g$  hole pockets is not surprising

at all because the  $e'_g$  band should be filled in the valence band further below both  $a_{1g}$  and  $b_{2g}$ , which is consistent with the description of a large inter-orbital repulsion  $U'$  proposed by Zhou *et al.*<sup>8</sup> The inconsistent  $a_{1g}-e'_g$  level splitting predicted from *ab initio* calculations and the octahedral CEF with trigonal distortion originated from the mislabeling of  $a_{1g}$  as shown in Fig. 3. The actual CEF should be viewed as unexpectedly weak ligands in the apical positions of a pseudo-octahedral CEF, and the best starting point of a CEF description is the square-planar CEF followed by an increasing inter-chain coupling between the edge-sharing square-planar chains. The actual narrow gap is between the  $a_{1g}$  (which belongs to the  $e_g$  group) and  $b_{2g}$  (which belongs to the  $t_{2g}$  group) levels, as illustrated in Fig. 3(c), following the standard crystal field labeling by symmetry.

#### ACKNOWLEDGMENT

We are grateful to Patrick A. Lee for many helpful discussions. FCC acknowledges support from NSC-Taiwan under project number NSC 101-2119-M-002-007. GJS acknowledges support from NSC-Taiwan under project number NSC 100-2112-M-002-001-MY3.

- 
- \* fcchou@ntu.edu.tw
- <sup>1</sup> D. J. Singh, Phys. Rev. B **61**, 13397 (2000).
  - <sup>2</sup> S. Landron and M. B. Lepetit, Phys. Rev. B **77**, 125106 (2008).
  - <sup>3</sup> I. Terasaki, Y. Sasago, and K. Uchinokura, Phys. Rev. B **56**, R12685 (1997).
  - <sup>4</sup> J. T. Hertz, Q. Huang, T. McQueen, T. Klimczuk, J. W. G. Bos, L. Viciu, and R. J. Cava, Phys. Rev. B **77**, 075119 (2008).
  - <sup>5</sup> K. Takada, H. Sakurai, E. Takayama-Muromachi, and F. Izumi, Nature, **422**, 53 (2003).
  - <sup>6</sup> F. C. Chou, J. H. Cho, and Y. S. Lee, Phys. Rev. B **70**, 144526 (2004).
  - <sup>7</sup> J. R. Sootsman, D. Y. Chung, and M. G. Kanatzidis, Angew. Chem. **48**, 8616 (2009).
  - <sup>8</sup> S. Zhou, M. Gao, H. Ding, P. A. Lee, and Z. Wang, Phys. Rev. Lett. **94**, 206401 (2005).
  - <sup>9</sup> C. Bernhard, A. V. Boris, N. N. Kovaleva, G. Khaliullin, A. V. Pimenov, L. Yu, D. P. Chen, C. T. Lin, and B. Keimer, Phys. Rev. Lett. **93**, 167003 (2004).
  - <sup>10</sup> M. Daghofer, P. Horsch, and G. Khaliullin, Phys. Rev. Lett. **96**, 216404 (2006).
  - <sup>11</sup> M. D. Johannes, I. I. Mazin, and D. J. Singh, Phys. Rev. B **71**, 205103 (2005).
  - <sup>12</sup> G. J. Shu, A. Prodi, S. Y. Chu, Y. S. Lee, H. S. Sheu, and F. C. Chou, Phys. Rev. B, **76**, 184115 (2007).
  - <sup>13</sup> Y. Wang, N. S. Rogado, R. J. Cava, and N. P. Ong, Nature, **423**, 425 (2003).
  - <sup>14</sup> J. L. Luo, N. L. Wang, G. T. Liu, D. Wu, X. N. Jing, F. Hu, and T. Xiang, Phys. Rev. Lett. **93**, 187203 (2004).
  - <sup>15</sup> J.-S. Rhyee, J. B. Peng, C. T. Lin, and S. M. Lee, Phys. Rev. B **77**, 205108 (2008).
  - <sup>16</sup> F.-T. Huang, M.-W. Chu, G. J. Shu, H. S. Sheu, C. H. Chen, L.-K. Liu, P. A. Lee, and F. C. Chou, Phys. Rev. B **79**, 014413 (2009).
  - <sup>17</sup> R. Janes and E. Moore, Metal-ligand bonds, Royal Society of Chemistry, 2004.
  - <sup>18</sup> J. D. Lee, Concise Inorganic Chemistry, 5th Ed., Blackwell Science, 1996.
  - <sup>19</sup> T. Moriya, Spin fluctuations in itinerant electron magnetism, Springer Series in Solid-State Sciences 56, (1985).
  - <sup>20</sup> L. Balicas, Y.-J. Jo, G. J. Shu, F. C. Chou, and P. A. Lee, Phys. Rev. Lett. **100**, 126405 (2008).
  - <sup>21</sup> G. J. Shu, F.-T. Huang, M.-W. Chu, J.-Y. Lin, P. A. Lee, and F. C. Chou, Phys. Rev. B **80**, 014117 (2009).
  - <sup>22</sup> H. -B. Yang, Z. Wang, and H. Ding, J. Phys.: Condens. Matter. **19**, 355004 (2007).